

An Adaptive Signal Processing Framework for PV Power Maximization

André A. Vidal · Vítor Grade Tavares ·
José C. Príncipe

Received: 8 March 2013 / Revised: 7 January 2015 / Accepted: 8 January 2015 /
Published online: 14 February 2015
© Springer Science+Business Media New York 2015

Abstract This paper discusses the possibility of using adaptive signal processing techniques for maximum power point tracking controllers, in order to extract peak power from individual photovoltaic modules. A new technique grounded on unsupervised Hebbian learning theory (maximum eigenvector of the output power) is presented, which works on-online and is capable of operating without a desired response. Important modifications were made to the generic Hebbian adaptation to accommodate the intrinsic feedback loop between the controller and the plant. Analytic derivation of the new update rule is presented, as well as stability analysis by means of Lyapunov theory. Simulation results showing its effectiveness are presented, as well as experimental results.

Keywords Adaptive maximum power point tracking · MPPT · Hebbian learning · PV optimization

1 Introduction

The solar module current–voltage (IV) characteristic is nonlinear, and the maximum power extracted relies on various factors such as insolation, temperature and load

A. A. Vidal (✉) · V. G. Tavares (✉)
INESC Technology and Science (INESC TEC), Faculty of Engineering of the University of Porto
(FEUP), Rua Dr. Roberto Frias, 378, 4200-465 Porto, Portugal
e-mail: andre.vidal@fe.up.pt

V. G. Tavares
e-mail: vgt@fe.up.pt

J. C. Príncipe
Computational NeuroEngineering Laboratory, University of Florida, Gainesville, FL, USA
e-mail: principe@cnel.ufl.edu

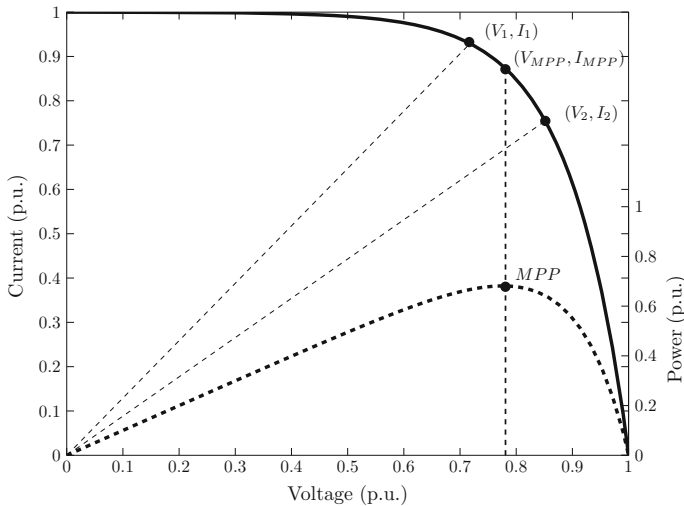
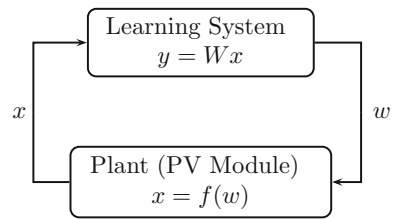


Fig. 1 Typical IV curve of a generic PV module. The corresponding power curve is shown in a strong dashed curve (note that the vertical scaling is different than that used in IV curve)

impedance. Therefore, there is a unique IV point, called the maximum power point (MPP), at which the PV system operates with maximum power, maximizing the produced energy, as shown in Fig. 1. To locate this optimum point, several MPPT techniques are used, following two approaches: indirect and direct methods. Indirect methods require the measurement of several variables such as voltage, current and/or environmental conditions, which are then fitted into an IV curve that has been modeled off-line [4, 10], or compared with IV values stored in the control system under concrete climatological conditions [6]. However, to obtain a reasonable MPP approximation, accurate knowledge of the PV physical parameters is required, large memory capacity is necessary, and therefore, the computational demands are significantly high. Other indirect methods assume that the IV characteristic is linear within a specific range, so by measuring either the open-circuit voltage or the short-circuit current, the MPP is given as a ratio of one of these measurements [1, 8]. Nevertheless, the system operation needs to be interrupted to make such measurements, yielding significant power losses. In general, indirect methods do not guarantee the optimum point and require previous knowledge of the PV characteristics.

Direct methods seek the MPP by taking into account the operating point variations, hill climbing the power curve, through time. Therefore, the search for the optimal point is made without previous knowledge of the panel or its environmental conditions. One of the most utilized techniques is the Perturb and Observe (P&O) method [5, 7, 11, 17], which periodically perturbs the terminal voltage and then moves it in the direction of the rate of change of power by a fixed and predetermined step. This iterative process reaches MPP when the rate of change is zero. A disadvantage of this method is that when a sudden increase of irradiance occurs, the algorithm assumes that the cause results from a previous perturbation and not from the characteristic change. The incremental conductance (IncCond) method [19] solves this problem by computing

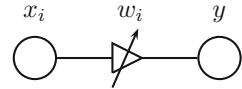
Fig. 2 Hebbian learning with weight feedback controller



the ratio between a change in current and voltage measurements. This ratio indicates then the direction of change in conductance, which is incremented (or decremented) with a predetermined step. Some more methods and variations of these exist, and the most recent ones make use of fuzzy logic and neural networks [2, 3, 13]. However, all of these methods measure at least two variables: the output current and voltage to compute the actual power. Some authors have also proposed a model where the current is the sole variable needed to reach the MPP, but this model can only be used for battery charging applications, since the converter output voltage is approximately fixed [14]. Comprehensive surveys can be found in [7, 16].

In general, all methods seek the optimum impedance “seen” from the PV terminals. These are connected to DC/DC power converters, which transfer power to a load. In order to change the impedance, the duty cycle of DC/DC power converters is varied to match, on average, the desired input impedance. This paper approaches this problem in an adaptive and scalable control perspective, where the learning system receives the plant state, x , and computes the new weight, w , which is connected to the external environment (the PV module) in closed loop, with the goal of maximizing the output power (Hebbian cost function). This way, the learning system is configured to optimize a criterion function that relates x and w , which is continuously differentiable and bounded. In the particular MPPT problem, it is evident that the cost function should follow the same shape as the actual PVs power curve and that the global maxima of both functions must coincide. Although the output signal y is computed, it is not directly used to control the plant. Yet, it is used by the weight adaptation, as in conventional Hebbian Learning. This feedback configuration, shown in Fig. 2, is unconventional in adaptive filtering applications, specifically the direct use of the weight as a control signal. Young and Poon [23] proposed a similar optimal control setup, using the an Hebbian type of covariance feedback learning scheme. Nonetheless, their approach effectively uses the learning system output y as a control signal.

This paper is organized as follows. Next section introduces some basic notions of the classic Hebbian Learning rule, and the possibility of using it to perform MPPT is discussed. Then, this rule is extended to optimize generic systems with weight feedback, presenting a generic modified Hebbian rule. Also, in this section, the particular learning rule to maximize the delivered power of PV modules is derived, as well as how to interface the adaptive system with the physical system—a PV panel controlled with an individual DC/DC converter. The final part of this section presents a stability analysis of the developed algorithm, proving that it is globally stable using Lyapunov Theory. In Sect. 3, it is shown through computer simulations that the proposed controller is effectively able to optimize the power delivered by a PV module, in a

Fig. 3 Linear unit model

robust fashion, even when abrupt changes (step) occur in its characteristic. Experimental results, presented in Sect. 4, confirm our expected results for a real PV module. Finally, Sect. 5 discusses the advantages of the method as well as comparison between simulation and experimental results.

2 Controller Architecture

2.1 Hebbian Theory Applied to MPPT

The Hebbian rule maximizes the output variance of a linear processing unit— $E[y^2]$, assuming y is zero mean, by altering the weights (w_i) [17], as shown in Fig. 3. The output is simply a linear combination of one or more inputs (x_i) and the weights (w_i), where i is the weight and input indexes. After convergence, the weight vector is aligned with the direction of the largest eigenvector of the input correlation matrix [12].

The update rule can easily be obtained by taking the derivative of $E[y^2]$, as shown in (1), where the expectation $E[\cdot]$ operator was dropped, because here we will be seeking a stochastic gradient approach. The direction of change should follow this gradient (increasing direction), which is the same as the formal rule represented in (2) (the scalar 2 is embedded in the step size constant η , controlled by the user).

$$\frac{\partial y^2}{\partial w} = \frac{\partial}{\partial w} (x^2 w^2) = 2wx^2 = 2xy \quad (1)$$

$$\Delta w_i = \eta x_i y \quad (2)$$

In practical applications, some form of normalization or nonlinearity must be used to stabilize the weights, otherwise they grow without bounds [9]. If a single input is considered, the output simply becomes $y = wx$. If one assigns to x , the square of the PV's measured voltage V_{pv} and the electrical conductance to w , this model is in fact optimizing the PV's delivered power, $V_{pv}^2 w$. Hence, the objective function is defined as:

$$J = (x \cdot w)^2 \quad (3)$$

Therefore, two systems must be considered: (1) the adaptive system that receives the present voltage measurement and, given the previously determined weight, estimates the output power of the panel; (2) the physical system that receives some input from the adaptive system and changes the panel operating point. One can easily conclude that such input should be the equivalent electrical conductance (or load) at the PV terminals. In this way, the controller is able to shift the actual PV state (IV point) to a different and more appropriate state. This effect is shown in Fig. 1, where two different

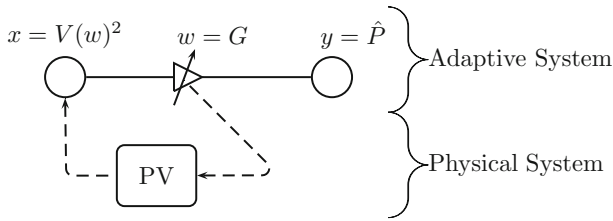


Fig. 4 System’s configuration

conductances place the PV at different operation points, therefore generating more (or less) power.

2.2 Recurrent Hebbian Learning Rule

Unfortunately, the simple generic Hebbian update rule shown in (2) cannot be used in this scenario as it is focused on feed-forward networks, where no feedback exists, i.e., normally the input signal x is independent of the adaptive system. In the proposed method, x is also a function of w , since a different conductance implies a different IV point, related with the particular PV characteristic. Therefore, this interaction must be taken into account in the update rule. Moreover, the cost function (J) must have a global maximum with respect to w , and its global maximum must satisfy w^* such that $p(w^*)$ is the maximum power point (being w^* the optimum conductance, and $p(w^*)$ the maximum power). This system architecture is depicted in Fig. 4. It is important to note that this configuration still follows the same concept of linear adaptive models, where the weights work as “knobs” to optimize a certain criterion function. Furthermore, the weights are naturally bounded (if convergence is assured) by the plant nonlinearity, avoiding normalization procedures such as Oja’s rule [18].

Under these circumstances, the objective function to be maximized is as shown in (4):

$$J = J(x(w), w) \tag{4}$$

The rate of change of the objective function, with respect to w , yields the update rule for the PV system. Thus, J is differentiated with respect to w :

$$\frac{dJ}{dw} = \frac{\partial J}{\partial x} \frac{dx}{dw} + \frac{\partial J}{\partial w} \tag{5}$$

Since for our problem, the objective function is still defined as the output power $J = y^2$, substituting in (5) yields

$$\frac{dJ}{dw} = 2w^2 \frac{dx(w)}{dw} x(w) + 2w(x(w))^2 \tag{6}$$

The weight is therefore updated proportionally to this gradient, yielding

$$w_{n+1} \leftarrow w_n + \eta [x_n y_n + w_n y_n d_n] \tag{7}$$

where $y_n = x_n w_n$, n is the iteration step, $\frac{dx}{dw}$ was replaced by d_n , a small proportionality constant η was included for step-size control, and the 2 scalar was aggregated in it. Note that the role of the adaptive system output (y) is now to provide an estimate of the current delivered power. This rule effectively maximizes the power delivered by an individual PV module, providing an on-line system identification method, although not complete identification is carried out, since it is not necessary. Through this gradient approach, the power curve is climbed with a variable step size so, as the MPP is being reached the step size is reduced. This way, η should be chosen so that a good trade-off exists between the speed of adaptation and steady-state oscillations (rattling). Its resulting expression resembles the conventional Hebbian rule shown in (2), with the addition of the plant feedback (reflected by the d_n derivative). The adaptation ends when these two terms cancel each other, reaching the MPP. This derivative can be approximated through temporal differences of x and w , as

$$d_n = \frac{x_n - x_{n-1}}{w_n - w_{n-1}} \quad (8)$$

The derivative estimation is of major importance, especially because when the algorithm reaches the optimum conductance w^* , its value is nonzero. In fact, by making $(w_n - w_{n-1}) = 0$ in (7) yields:

$$d^* = -\frac{x^*}{w^*} \quad (9)$$

where d^* , x^* and w^* refer to the optimum values for the respective variables. Here, we apply smooth derivative operators, as follows:

$$d(t) = \frac{x(t) - \int_{t-T}^t x(t) dt}{w(t) - \int_{t-T}^t w(t) dt} \quad (10)$$

where T is the period of this moving average filter.

2.3 Stability Analysis

The update rule just derived can be written in terms of the time derivative of w , as follows:

$$\dot{w} = f(w) \quad (11)$$

where $(\dot{\cdot})$ refers to the time derivate of the respective variable and

$$f(w) \simeq \frac{\eta}{T} \frac{dJ}{dw} \quad (12)$$

where T is the sampling step of the controller (note that when $T \rightarrow 0$, this approximation becomes exact). Also, note that the dynamics of an hypothetical DC/DC converter attached to the PV module are neglected. We are now ready to prove asymptotic convergence.

Theorem 1 *The autonomous system in (11) is globally stable around a nominal motion—the optimum power point.*

The proof will be conducted through the Lyapunov direct method, by transforming it as a stability problem around the origin of the equivalent system.

Proof Let the error between the optimum conductance w^* and the present one be defined as $e(t) = w(t) - w^*$. Therefore, the goal is to study the following autonomous system with respect to the origin:

$$\begin{aligned}\dot{e} &= g(e) \\ &= f(w^* + e) - f(w^*)\end{aligned}\quad (13)$$

Let $V(e)$ be a Lyapunov candidate function for this system. It will now be shown that the conditions for global stability are satisfied for that function, thus proving global stability of the system. In other words, $V(e)$ is a positive-definite function and $\dot{V}(e)$ is negative-definite function for the given system. Let such function be defined as:

$$V(e) = \frac{T}{4\eta} e^2 \quad (14)$$

This function is positive definite. Note that it was considered that T is to be small enough to make both sides of Eq. (12) equal. Taking its derivative with respect to time, one obtains:

$$\begin{aligned}\dot{V}(e) &= \frac{T}{2\eta} e \dot{e} \\ &= \frac{T}{2\eta} e (f(w^* + e) - f(w^*)) \\ &= e \left(\left[x(w)^2 w + w^2 x(w) \frac{dx}{dw}(w) \right] \Big|_{w=w^*+e} - 0 \right)\end{aligned}\quad (15)$$

The terms of this equation can be aggregated into:

$$\dot{V}(e) = \left(ex(w)w \frac{d[x(w)w]}{dw} \right) \Big|_{w=w^*+e} \quad (16)$$

For an easier reading, consider the three terms of the equation: the e factor, $x(w)w$ and $\frac{d[x(w)w]}{dw}$ all evaluated at $w = w^* + e$. The second term is a translated version of the power curve in the e domain by w^* , i.e., $y(w^* + e)$. It is always positive within the domain of interest, i.e., $\forall e > -w^*$ (note that for $e < -w^*$, the w value becomes negative, which will never occur because w always acts as a passive resistor load). The third term is the derivative of the power (y) with respect to w evaluated at $w^* + e$, and hence, its value is zero when $e = 0$. One can study how such function behaves, by looking at the $y(w)$ function. Note that, when $w = 0$, the PV operates in open circuit, and hence, the delivered power is zero. Conversely, if $w = \infty$, the PV operates in short circuit, also delivering zero power. In the e domain, these two values correspond

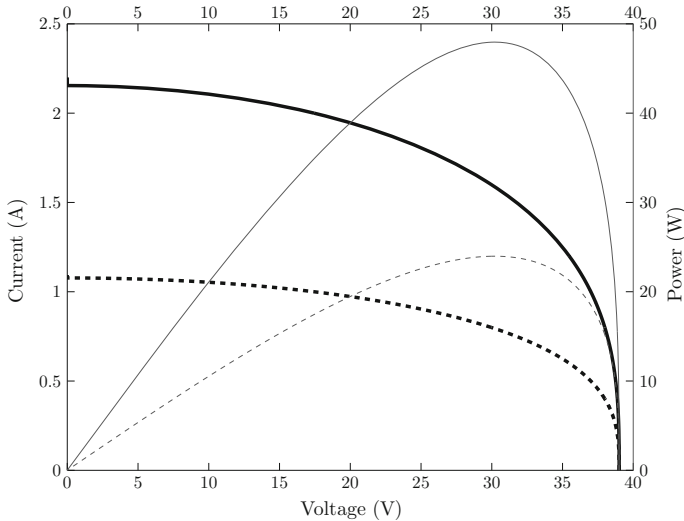


Fig. 5 Current–voltage curve and respective power voltage of the simulated PV module used to compare the developed method with the P&O method. The *dashed curves* correspond to the same PV module but when the irradiance has been reduced to half

to $e = -w^*$ and $e = \infty$, respectively. For $e = 0$, its value is maximum; therefore when $e \in [-w^*, 0[$, the corresponding derivative is positive and when $e \in]0, \infty[$, the derivative is negative. This observation provides a sufficient proof of stability, since we have shown that: 1) when $e \in [-w^*, 0[$ all terms in $\dot{V}(e)$ are positive, but the e factor implies that this equation takes a negative value; 2) when $e \in]0, \infty[$, all terms are positive expect for the third one yielding a negative function; 3) $\dot{V}(0) = 0$. \square

The main conclusion of this proof is that, provided that the $\frac{dx}{dw}$ derivative (implemented using Eq. (8)) is properly estimated, the controller is able to “force” the connected PV module to operate at its MPP.

3 Simulations

In order to test the effectiveness of the proposed technique, the system was modeled in the MATLAB/Simulink environment so that different scenarios could be tested.

In order to effectively impose the conductance computed by the adaptive controller, some sort of interface system must be employed between the adaptive system and the DC/DC converter, translating the conductance value into an equivalent duty-cycle value. Assuming an ideal converter, this could be done by using the known input/output resistance relations for this type of converter. However, the output load would have to be known, which in most practical situations is unknown. To address this problem, a PI controller was introduced to adjust the duty cycle based on the error signal determined between the input resistance returned by the controller and the actual input resistance.

Two sets of simulation tests were conducted. In the first scenario, the algorithm was compared with the P&O and IncCond methods, since they are perhaps the most fre-

quently found algorithms in literature. The controlling variable in these two algorithms is the voltage value, which is later fed into a PI controller, imposing it at the PV terminals. Conceptually, the controllers' procedure is similar to the developed algorithm, i.e., a new value of an electric variable is computed and a PI controller adjusts the duty cycle, so that the present and the desired values match. To achieve proper performance comparison, the system to be optimized was kept exactly the same throughout the various simulations. The simulated PV module was based on the one-diode model, whose characteristic curve is as shown in Fig. 5 (represented by the solid curves) and the system setup comprised the following characteristics: an MPPT update rate of 100 ms, a digital PI controller updated every 50 ms and a digital first-order low-pass filter running at 125 kHz, applied using:

$$y[n] = y[n - 1] + \alpha(x[n] - y[n - 1]) \quad (17)$$

where $y[n]$ is the output of the filter, $x[n]$ is the input and α is the smoothing factor, set to 0.1. It was applied to voltage, current and power signals, and the impedance value was further calculated throughout time. The relatively slow update rates of the different blocks are related to the relatively long time constant of the boost DC/DC converter, which had the following characteristic values: $L = 600\mu\text{H}$, $C = 1.080\text{ mF}$, being operated by a resistive load of value $R = 140\Omega$. It should be noted that the update rates were selected, so that they are large enough when compared to the relatively long time constant of the converter, thus neglecting the converter dynamics.

Regarding the derivative estimation in Eq. (8), the discrete version of the expression in Eq. (10) was used with a window of size 4 ($T = 400\text{ms}$ in the continuous version), followed by a saturation block. It avoids the high-frequency components present at the panel voltage, consequent of the converter switching, and also the spikes and large variations on the derivative estimate (d_n). A good choice for the upper and lower limits of this saturation function can be obtained using Eq. (9) as follows. It was assumed that in a real application, the optimum values (x^* and w^*) are not exactly known. Yet, one can easily obtain an ε value that bounds it, such that $\varepsilon > |d^*|$. A proper estimate can be accomplished by using the open-circuit voltage squared as x^* in nominal conditions (assumed known a-priori) and a moderately high value for the optimum conductance (w^*). In the simulation results, ε was set to 5×10^4 , which is considerably higher than the optimum value for this PV ($d^* = -1.7 \times 10^4$). The block diagram shown in Fig. 6 represents a simplified schematic of this setup.

In order to effectively compare the performance of both controllers, the step sizes were set so that the time constant of adaptation is approximately the same. Therefore, all were initialized with an input impedance of 100Ω , and the ΔV value was set to 1.5V for the P&O and IncCond algorithms. Regarding the developed algorithm, the step size (η) was set to 4.7×10^{-6} , leading to a convergence time of approximately 0.4 s for all the three algorithms.

Figure 7 shows the simulation results when the P&O algorithm was used; (a) shows the power extracted over time, while (b) displays the resistance and duty cycle, in blue and green, respectively. The optimum power and resistance values are shown in a horizontal, dashed red line for both plots.

Figure 8 shows analogous results, but now when the IncCond method was applied.

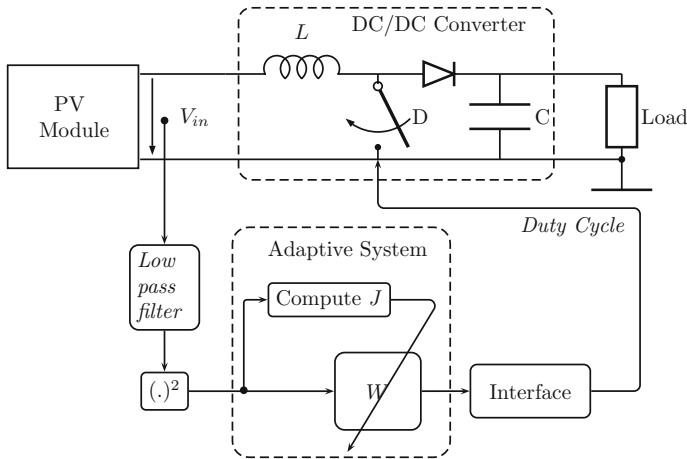


Fig. 6 Block diagram of the whole system

Finally, Fig. 9 shows the obtained results when the developed algorithm is applied to the same system. One thing that becomes immediately clear after comparison is the much smaller ripple present in steady state, for the same settling time of the algorithm. This effect is clearer in the resistance plot (note that both plots are in the same scale). This leads to a decrease on the average power extracted from the PV module.

The second test aimed at validating the designed algorithm against abrupt changes in the environment. A step change has been simulated in the irradiance, leading to a new IV characteristic for the attached module, which is shown in the dashed lines of Fig. 5. Here, the irradiance has been reduced to half, implying that the maximum extractable power is half of the nominal. Figure 10 shows the simulation results for this scenario (note that the step change occurred at $t = 1.5$ s). As expected, the algorithm is perfectly capable of tracking such change.

The most significant result from this section is that the proposed algorithm is effectively able to deliver, on average, more power than two of the most commonly found algorithms in the literature, P&O and IncCond. The benchmarking scenario resulted in the following average power extracted: 47.01W for P&O, 46.69W for IncCond and 47.67W for the presented algorithm, representing around 2% less power extraction when compared to the proposed algorithm.

4 Experimental Results

In order to confirm the results obtained during simulations, a simple prototype of the system was built. It comprises a dedicated DC/DC boost converter whose characteristics are exactly the same as those used in simulations. It was specially designed for this purpose, similar to the one represented in Fig. 6, controlled by the algorithm that is run by a PC application interfacing via RS232 port. Figure 11 shows this experimental implementation.

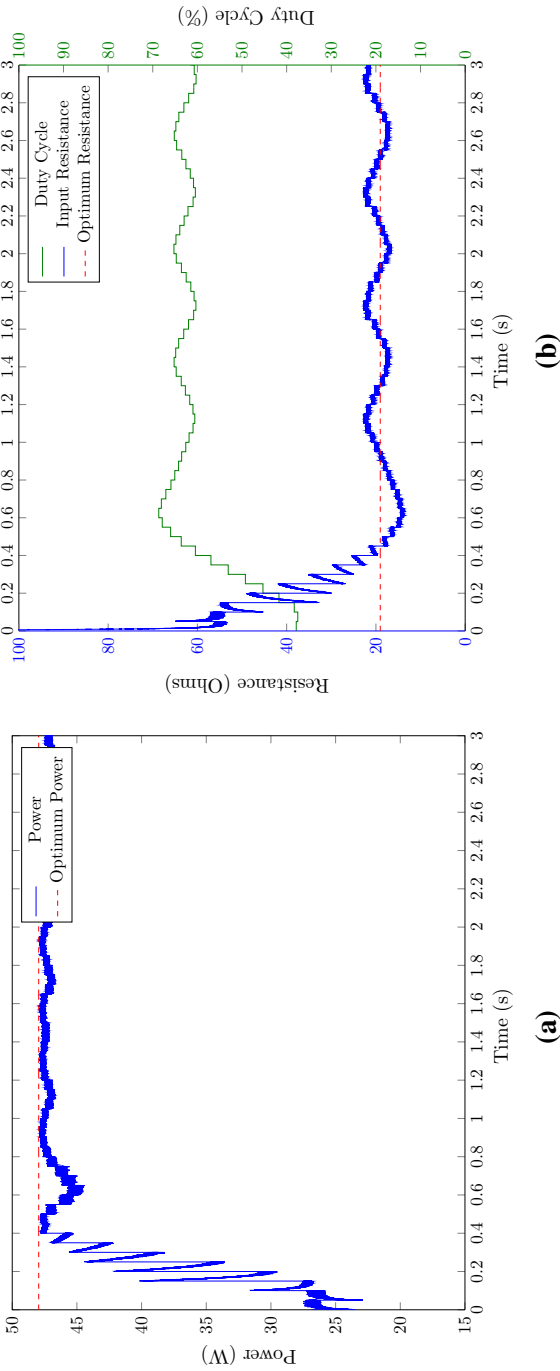


Fig. 7 Results for the P&O algorithm during simulations, using $\Delta V = 1.5V$. **a** Measured output power, **b** measured resistance (in blue) and duty cycle (in green) (Color figure online)

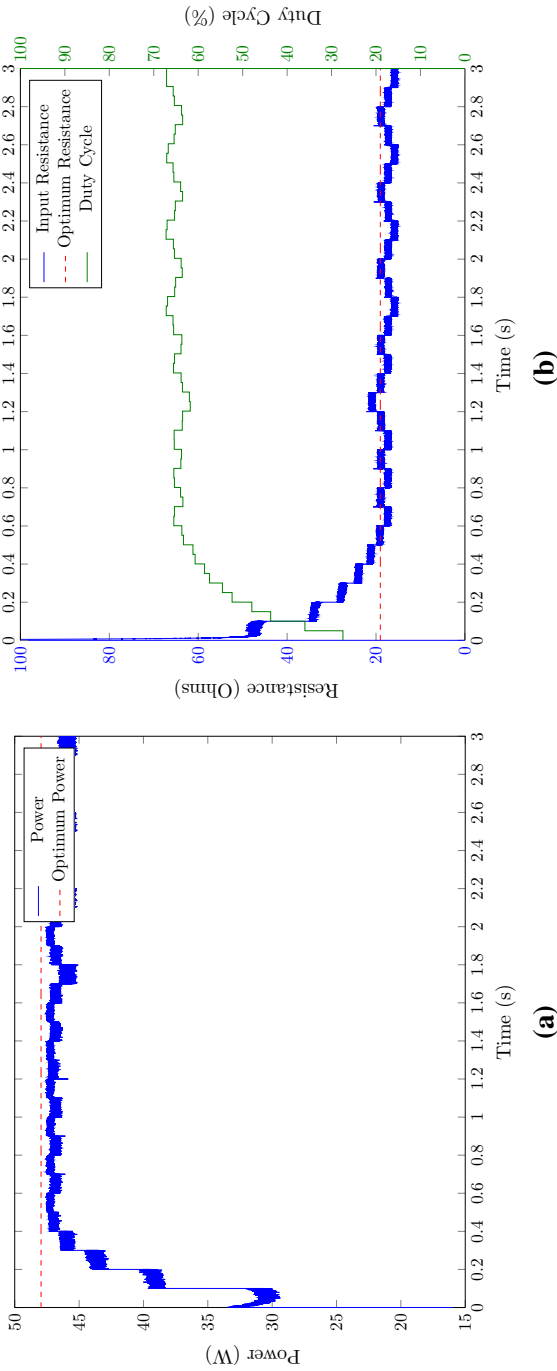


Fig. 8 Results for the IncCond algorithm during simulations, using $\Delta V = 1.5V$. **a** Measured output power, **b** measured resistance (in blue) and duty cycle (in green). The thicker black line displays the resistance set point (used by the PI) controller (Color figure online)

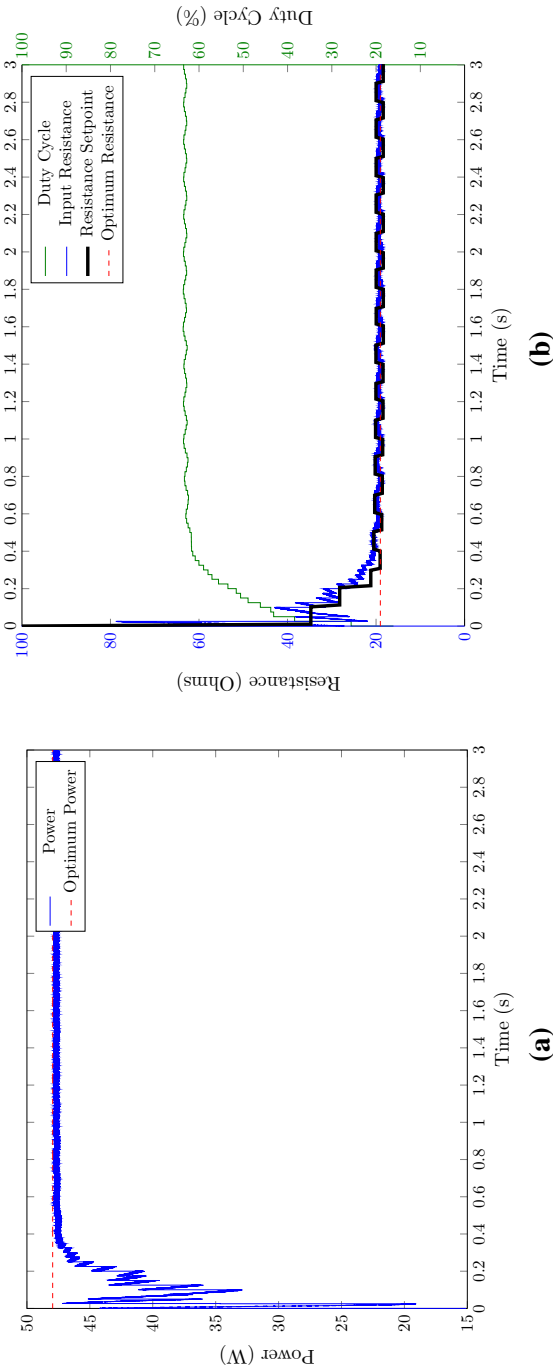


Fig. 9 Simulation results of the developed algorithm using $\eta = 4.7 \times 10^{-6}$. **a** Measured output power, **b** measured resistance (in blue) and duty cycle (in green). The thicker black line displays the resistance set point (used by the PI) controller (Color figure online)

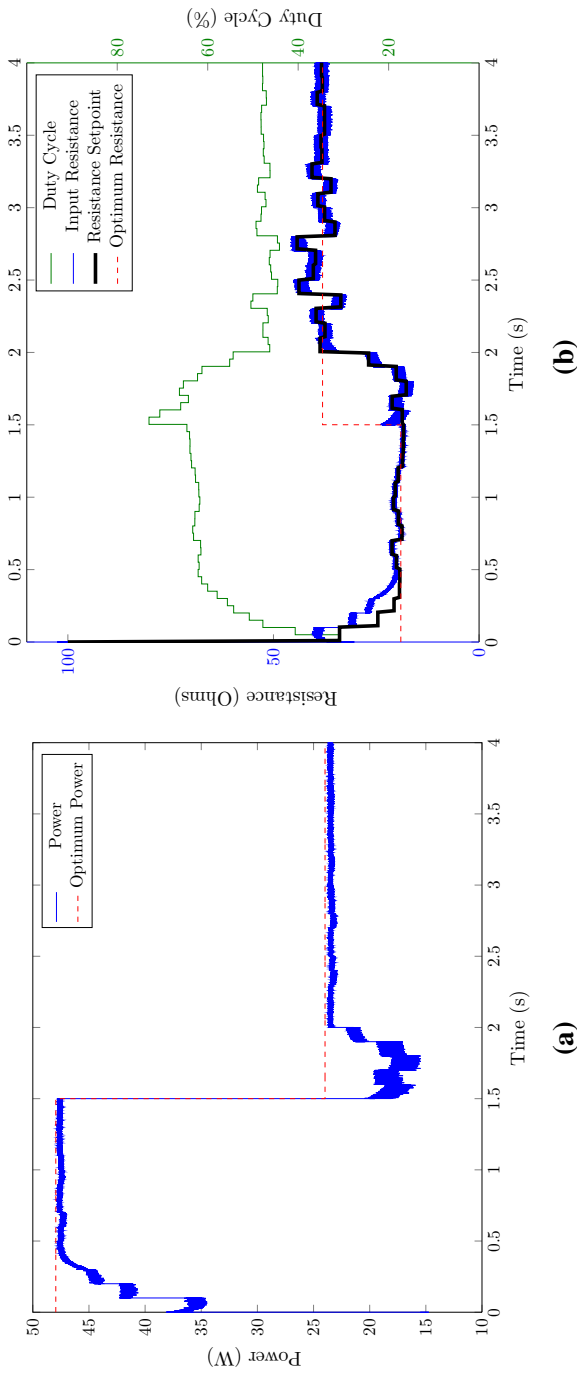


Fig. 10 Simulation results of the developed algorithm when a step change in the irradiance of the PV module occurred at 1.5s. ($\eta = 6 \times 10^{-6}$). **a** Measured output power, **b** measured resistance (in blue) and duty cycle (in green). The thicker black line displays the resistance set point (used by the PI) controller (Color figure online)

Fig. 11 DC/DC boost prototype built in your experiments



The data are collected by an ATMEL Atmega8 microcontroller, which simultaneously reads the electric signals through its internal 8 bit ADC at a sampling rate of $F_s = 125$ kHz. It also generates a 100 kHz rectangular wave, with variable duty cycle, to control the DC/DC switch (connected to a driver circuit that controls the MOSFET gate), as in simulations. On the PC side, a dedicated application was developed on the Lazarus Free-Pascal IDE environment that receives the electric measurements and implements the adaptation algorithm. A simple digital first-order low-pass digital filter was also applied with exactly the same characteristics of that used in the previous section.

A PI controller block is also implemented at this level, for the conductance loop. Apart from the adaptation algorithm, this application also returns the panel curve, when needed, sweeping the duty cycle of the PWM throughout all its operational range. The software keeps a log of the system state (voltage, current, power, etc.), so that one can later analyze the overall system. Figure 12 shows an image of the developed software running on a PC after an IV curve has been extracted (allowing adequate knowledge of the optimum values for the different variables prior to the algorithm execution). All the update rates were set exactly as in the simulations.

The system was tested in a clear sky day in order to avoid short-time changes in the PV's IV characteristic. Thus, the experimental procedure started by first extracting the PV curve, in order to obtain the optimum operating point. Next, the algorithm was allowed to run normally, logging the data over time. Figure 13 shows the IV and power curves of the real PV module used in the experimental setup. Based on this curve, the optimum operating points of the system are as follows: $V^* = 32.45$ V, $P^* = 53.62$ W, $R_{in}^* = 16.64$ Ω and $w^* = 0.050$. Note that the load connected at the DC/DC converter output terminals was considered to be large enough (140 Ω) when compared to the optimum resistance, allowing the controller to obtain a sufficiently complete range of the IV curve.

Figure 14 shows the experimental results of the algorithm running with $\eta = 2 \times 10^{-7}$, starting again with an input impedance of 100 Ω . The saturation limits for the derivative estimate were obtained as explained in the previous section, set now to $\varepsilon = 8 \times 10^4$. Here, the step size was significantly increased with respect to that used

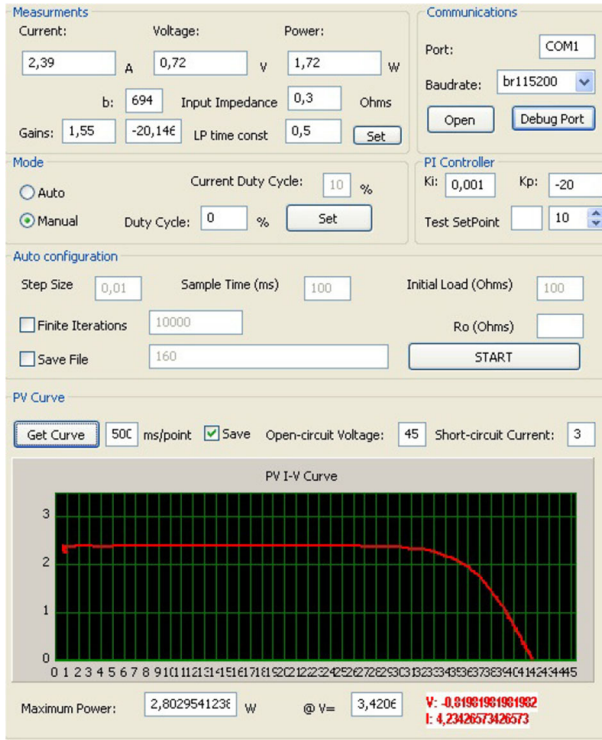


Fig. 12 Overview of the developed software after an I–V curve has been extracted from the connected PV

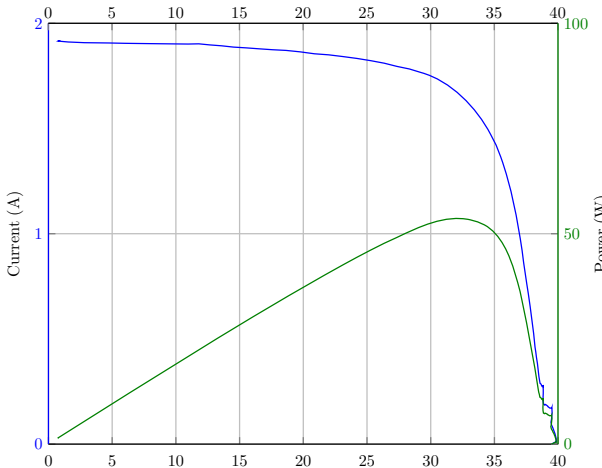


Fig. 13 Power and I–V curve of the PV module used in the experimental work

in the simulations, because of the larger noise magnitude present in the measured variables, mainly related to the used current sensor. However, similar conclusions can be drawn, confirming the results obtained during simulations. Despite having

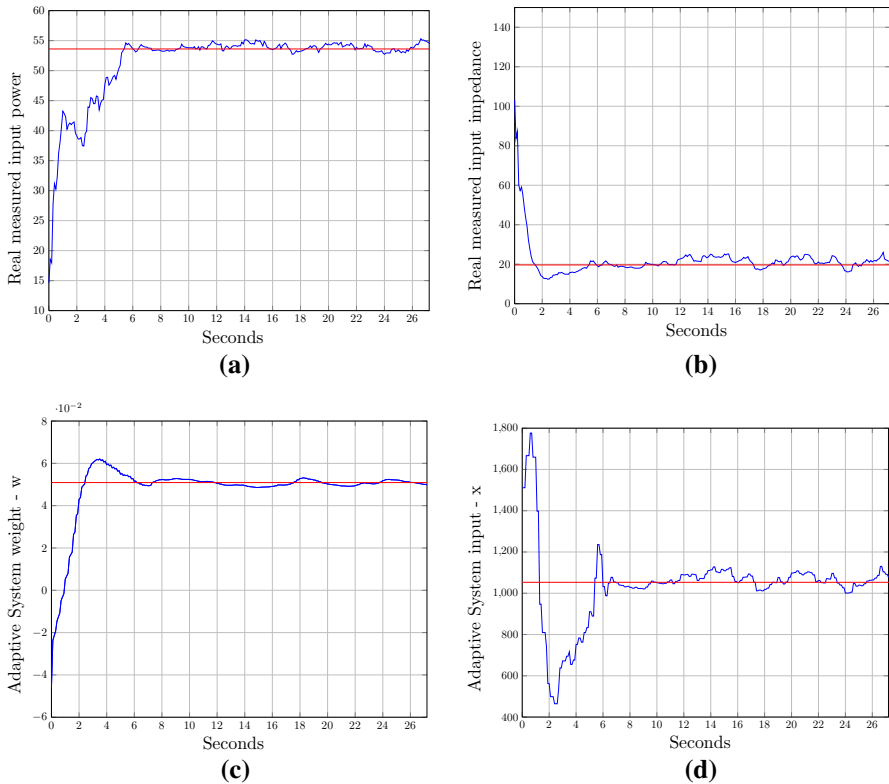


Fig. 14 Measured variables during the adaptation of a real PV module with the developed algorithm. **a** Measured output power, **b** measured resistance, **c** adaptive system weight (imposed conductance), **d** adaptive system input (measured voltage squared)

some *overshooting* at 2s, the algorithm quickly senses it, reaching steady state at approximately 6s.

5 Conclusions

This paper provides a methodology to perform MPPT in individual PV modules based on Hebbian Learning, mimicking the adaptive process carried out in Hebbian networks, i.e., tracking the largest eigenvectors of the input correlation matrix. Therefore, the application of adaptive signal processing methodologies to a control problem is by itself a contribution of this manuscript. Such paradigm leads to a weight feedback constraint, which is not normally present in these methodologies. It is shown how to modify the generic Hebbian rule to optimize these systems. A generic expression was also derived to obtain a learning rule that optimizes an arbitrary criterion function, which here has been applied to maximize the power output of PV modules. Along with this, stability analysis was also carried out using Lyapunov theory applied to a generic PV function, where a theoretical proof of global stability was presented. It

should be noted that, although focused on MPPT controllers, this methodology may be applied to any black-box device, where one wants to extract full power (provided that its function is differentiable and bounded).

Simulation and experimental results show that the method provides a robust alternative to perform MPPT in PV modules, especially when compared to two of the most usually found algorithms in real-life applications, P&O and IncCond. In fact, when optimizing individual panels, the proposed adaptation expression may resemble that of IncCond. However, it should be highlighted that as opposed to IncCond, the controller is in fact only utilizing a single variable (voltage) to perform adaptation, despite the fact that the impedance still needs to be set at the converter level. Yet, it is capable of extracting, on average, more power in steady state than that extracted by the two other algorithms, when the same settling time is considered. Although various methods have been proposed to increase the performance of these two algorithms, e.g., reducing ΔV as the controller is reaching the optimum, it was opted to test the controllers in their most basic form, since such approaches could also have been adopted to the developed algorithm. It should be also highlighted that although the developed methodology has been applied to a DC/DC converter in a *boost* typology, it can be used in any converter typology.

The developed method is based on strong theoretical foundations, grounded on an adaptive signal processing framework. This way, the presented framework may also open new perspectives on distributed MPPTs systems. It should be easily extended to incorporate the information of other panels in an aggregation with the purpose to control the overall power. As in conventional adaptive systems, the output of the controller will be the weighted sum of the inputs (other panels' state), and the weights will still be related to the duty cycle of each associated converter in a certain way. Thus, the output is still the estimated power delivered, but now in global terms. The proposed method has no *prior* information regarding the model itself. In this sense, it is similar to data-driven frameworks, which operate only based on data gathered from sensors. Examples of its application [20–22] have shown to produce exciting results. Regarding a practical implementation of the learning rule itself, the only required free parameter to be set is the step size (η). This has direct implication in the time of convergence of the system and steady-state *rattling*. It also influences the estimation of the voltage-conductance derivative (d_n). A poor estimation of such value might worsen the global performance considerably. As future research work, we aim at studying the performance and robustness gains of using H_∞ [15, 18] methods in either a single or multi-PV framework.

Acknowledgments This work is supported by the ERDF through the Programme COMPETE and by the Portuguese Government through FCT—Foundation for Science and Technology, project ref. CMU-PT/SIA/0005/2009. The authors would also like to thank the “Autonomia Recursos Renováveis, SA” company for providing the PV module used in the experimental work.

References

1. J. Ahmad, A fractional open circuit voltage based maximum power point tracker for photovoltaic arrays, in *2010 2nd International Conference on Software Technology and Engineering (ICSTE)*, vol. 1, pp. V1-247–V1-250 (2010). doi:[10.1109/ICSTE.2010.5608868](https://doi.org/10.1109/ICSTE.2010.5608868)

2. F. Bouchafaa, D. Beriber, M. Boucherit, Modeling and simulation of a grid connected pv generation system with mppt fuzzy logic control, in *2010 7th International Multi-Conference on Systems Signals and Devices (SSD)*, pp. 1–7 (2010). doi:[10.1109/SSD.2010.5585530](https://doi.org/10.1109/SSD.2010.5585530)
3. A. Chaouachi, R. Kamel, K. Nagasaka, Microgrid efficiency enhancement based on neuro-fuzzy mppt control for photovoltaic generator, in *2010 35th IEEE Photovoltaic Specialists Conference (PVSC)*, pp. 002889–002894 (2010). doi:[10.1109/PVSC.2010.5614462](https://doi.org/10.1109/PVSC.2010.5614462)
4. G. Farivar, B. Asaei, M. Rezaei, A novel analytical solution for the pv-arrays maximum power point tracking problem, in *2010 IEEE International Conference on Power and Energy (PECon)*, pp. 917–922 (2010). doi:[10.1109/PECON.2010.5697710](https://doi.org/10.1109/PECON.2010.5697710)
5. N. Femia, G. Petrone, G. Spagnuolo, M. Vitelli, Optimization of perturb and observe maximum power point tracking method. *IEEE Trans. Power Electron.* **20**(4), 963–973 (2005). doi:[10.1109/TPEL.2005.850975](https://doi.org/10.1109/TPEL.2005.850975)
6. H.S. Ibrahim, F. Houssiny, H. El-Din, M. El-Shibini, Microcomputer controlled buck regulator for maximum power point tracker for dc pumping system operates from photovoltaic system, in *Fuzzy Systems Conference Proceedings, 1999. FUZZ-IEEE '99*. 1999 IEEE International, vol. 1, pp. 406–411 vol. 1 (1999). doi:[10.1109/FUZZY.1999.793274](https://doi.org/10.1109/FUZZY.1999.793274)
7. R. Leyva, C. Alonso, I. Queinsec, A. Cid-Pastor, D. Lagrange, L. Martinez-Salamero, Mppt of photovoltaic systems using extremum-seeking control. *IEEE Trans. Aerosp. Electron. Syst.* **42**(1), 249–258 (2006). doi:[10.1109/TAES.2006.1603420](https://doi.org/10.1109/TAES.2006.1603420)
8. T. Noguchi, S. Togashi, R. Nakamoto, Short-current pulse-based maximum-power-point tracking method for multiple photovoltaic-and-converter module system. *IEEE Trans. Ind. Electron.* **49**(1), 217–223 (2002). doi:[10.1109/41.982265](https://doi.org/10.1109/41.982265)
9. E. Oja, Simplified neuron model as a principal component analyzer. *J. Math. Biol.* **15**(3), 267–273 (1982). doi:[10.1007/BF00275687](https://doi.org/10.1007/BF00275687)
10. M. Park, I.K. Yu, A study on the optimal voltage for mppt obtained by surface temperature of solar cell, in *30th Annual Conference of IEEE on Industrial Electronics Society, 2004. IECON 2004*, vol. 3, pp. 2040–2045 (2004). doi:[10.1109/IECON.2004.1432110](https://doi.org/10.1109/IECON.2004.1432110)
11. L. Piegari, R. Rizzo, Adaptive perturb and observe algorithm for photovoltaic maximum power point tracking. *IET Renew. Power Generat.* **4**(4), 317–328 (2010). doi:[10.1049/iet-rpg.2009.0006](https://doi.org/10.1049/iet-rpg.2009.0006)
12. J.C. Principe, N.R. Euliano, W.C. Lefebvre, *Neural and Adaptive Systems: Fundamentals Through Simulations* (Wiley, New York, 2000)
13. R. Ramaprabha, B. Mathur, M. Sharanya, Solar array modeling and simulation of mppt using neural network, in *2009 International Conference on Control, Automation, Communication and Energy Conservation, 2009, INCACEC 2009*, pp. 1–5 (2009)
14. V. Salas, E. Olas, A. Lzaro, A. Barrado, New algorithm using only one variable measurement applied to a maximum power point tracker. *Solar Energy Mater. Solar Cells* **87**(1–4), 675–684 (2005). doi:[10.1016/j.solmat.2004.09.019](https://doi.org/10.1016/j.solmat.2004.09.019). URL <http://www.sciencedirect.com/science/article/pii/S092702480400385X>. International Conference on Physics, Chemistry and Engineering
15. B. Shen, Z. Wang, X. Liu, A stochastic sampled-data approach to distributed filtering in sensor networks. *IEEE Trans. Circuits Syst. I Regular Pap.* **58**(9), 2237–2246 (2011). doi:[10.1109/TCSI.2011.2112594](https://doi.org/10.1109/TCSI.2011.2112594)
16. Shmilovitz D., L.Y.: Distributed maximum power point tracking in photovoltaic systems—emerging architectures and control methods. *Automatika? J. Control Meas. Electron. Comput. Commun.* **53**(2), 142–155 (2012)
17. C.W. Tan, T. Green, C. Hernandez-Aramburo, Analysis of perturb and observe maximum power point tracking algorithm for photovoltaic applications, in *IEEE 2nd International Power and Energy Conference, 2008, PECon 2008*, pp. 237–242 (2008). doi:[10.1109/PECON.2008.4762468](https://doi.org/10.1109/PECON.2008.4762468)
18. Z. Wang, B. Shen, H. Shu, G. Wei, Quantized control for nonlinear stochastic time-delay systems with missing measurements. *IEEE Trans. Autom. Control* **57**(6), 1431–1444 (2012). doi:[10.1109/TAC.2011.2176362](https://doi.org/10.1109/TAC.2011.2176362)
19. Z. Xuesong, S. Daichun, M. Youjie, C. Deshu, The simulation and design for mppt of pv system based on incremental conductance method, in *2010 WASE International Conference on Information Engineering (ICIE)*, vol. 2, pp. 314–317 (2010). doi:[10.1109/ICIE.2010.170](https://doi.org/10.1109/ICIE.2010.170)
20. S. Yin, S. Ding, A. Abandan Sari, H. Hao, Data-driven monitoring for stochastic systems and its application on batch process. *Int. J. Syst. Sci.* **44**(7), 1366–1376 (2013). doi:[10.1080/00207721.2012.659708](https://doi.org/10.1080/00207721.2012.659708)

21. S. Yin, S.X. Ding, A. Haghani, H. Hao, P. Zhang, A comparison study of basic data-driven fault diagnosis and process monitoring methods on the benchmark tennessee eastman process. *J. Process Control* **22**(9), 1567–1581 (2012). doi:[10.1016/j.jprocont.2012.06.009](https://doi.org/10.1016/j.jprocont.2012.06.009)
22. S. Yin, H. Luo, S. Ding, Real-time implementation of fault-tolerant control systems with performance optimization. *IEEE Trans. Ind. Electron.* **61**(5), 2402–2411 (2014). doi:[10.1109/TIE.2013.2273477](https://doi.org/10.1109/TIE.2013.2273477)
23. D.L. Young, C.S. Poon, A hebbian feedback covariance learning paradigm for self-tuning optimal control. *Trans. Syst. Man Cyber. Part B* **31**(2), 173–186 (2001). doi:[10.1109/3477.915341](https://doi.org/10.1109/3477.915341)